COMMENTARY

Check for updates

A reflection on 'Size-tunable rhodium nanostructures for wavelength-tunable ultraviolet plasmonics'

Zhijia Geng and Jie Liu (ID) *

Plasmonic photocatalysis presents a novel approach for controlling heat and light, enabling reactions to take place under milder conditions. In 2016, Zhang and co-workers reported a novel approach in synthesizing rhodium nanocubes with desired sizes and surface plasmon resonances frequency, where the resonance frequency underwent a red-shift from deep UV to 400 nm as the size increased (X. Zhang, P. Li, Á. Barreda, Y. Gutiérrez, F. González, F. Moreno, H. O. Everitt and J. Liu, *Nanoscale Horiz.*, 2016, **1**, 75–80, https://doi.org/10.1039/C5NH00062A). In this reflection, we discuss the impact of this work and summarize the research inspired by this initial discovery.

Over the last decade, plasmonic photocatalysis has been extensively studied. Researchers mostly focused on Au and Ag nanoparticles (NPs) as plasmonic photocatalysts, and their resonant frequencies are confined to the visible and near-infrared regions.[1] As ultraviolet-excited nanostructures, rhodium NPs are synthesized from the stable noble metal that enhances applications in UV plasmonics.[2,3] The excitation of the collective electron oscillation on the rhodium NP and the generation of concentrated electromagnetic fields near the NP surface are described as localized surface plasmon resonance (LSPR). The following radiative decay leads to the surface-enhanced Raman scattering (SERS), and the non-radiative decay brings electron–hole pair separation and increased lattice temperature.[4]

Our interest in Rh and UV plasmonics was first established by earlier work in 2015, where the synthesized Rh nanotripods with attached *p*-aminothiophenol (PATP) exhibited local field enhancement and charge transfer processes upon UV light excitation.[5] We observed an enhanced Raman signal from PATP by a

factor of 3 under UV excitation compared to <1.5 under visible light. However, most existing synthesis methods produce polydisperse mixtures of tripods and tetrapods with uncontrollable size distributions.[6] Moreover, some other Rh nanocomposites only exhibit deep UV excitation.[7] Therefore, in 2016, in the first issue of *Nanoscale Horizons*, we published an article entitled "Size-tunable rhodium nanostructures for wavelength-tunable ultraviolet plasmonics" (https://doi.org/10.1039/C5NH00062A).[8] We developed two innovative slow-injection polyol methods, seeded and unseeded, to synthesize Rh nanocubes (NC) with controlled size and shape. The concentration of generated Rh atoms and the Rh precursor controlled the size of the synthesized NCs. Using the unseeded method, we synthesized particles with edge lengths of 15, 21, and 27 nm by varying the reaction time (Fig. 1b–d). The Rh NCs with the 27 nm edge length were used directly as seeds for the seeded synthesis method to synthesize the Rh NCs with edge lengths between 27 and 59 nm (Fig. 1f–h). The synthesized Rh NCs were tested under UV-vis extinction spectroscopy (Fig. 1a and e), and the LSPR peaks were measured (Fig. 1j). As the edge length of the NC increased, the

energy extinction decreased, and the excitation wavelength experienced a red shift toward the lower edge of the UV spectrum. Upon UV light illumination, the concentrated high-energy fields and hot electrons from the Rh NCs could be significant sources for photochemical reactions, demonstrating an enhanced Raman signal with PATP coating and efficient photodegradation abilities.

With a solid understanding of the plasmonic light interaction on the synthesized Rh NCs, we further explored their plasmonic photocatalysis behaviors in CO_2 reduction.[9] The Rh NCs with an edge length of 37 nm were synthesized based on our published *Nanoscale Horizons* paper and dispersed on Al_2O_3, serving as a photocatalyst placed in a fixed-bed Harrick reaction chamber. Under UV illumination, high selectivity in producing CH_4 on Rh/Al_2O_3 or CO on Au/Al_2O_3 was observed (Fig. 2a and b). Controlled experiments using pure Al_2O_3 and isotopic labelling confirmed that CH_4 and trace amounts of CO from Rh/Al_2O_3 were generated by Rh NCs instead of the Al_2O_3 support or contaminants. This highlights the primary role of plasmonic nanoparticles in these reactions. Further experiments testing the production rate over a selected heating temperature

Department of Chemistry, Duke University, Durham, North Carolina 27708, USA. E-mail: jliu@duke.edu
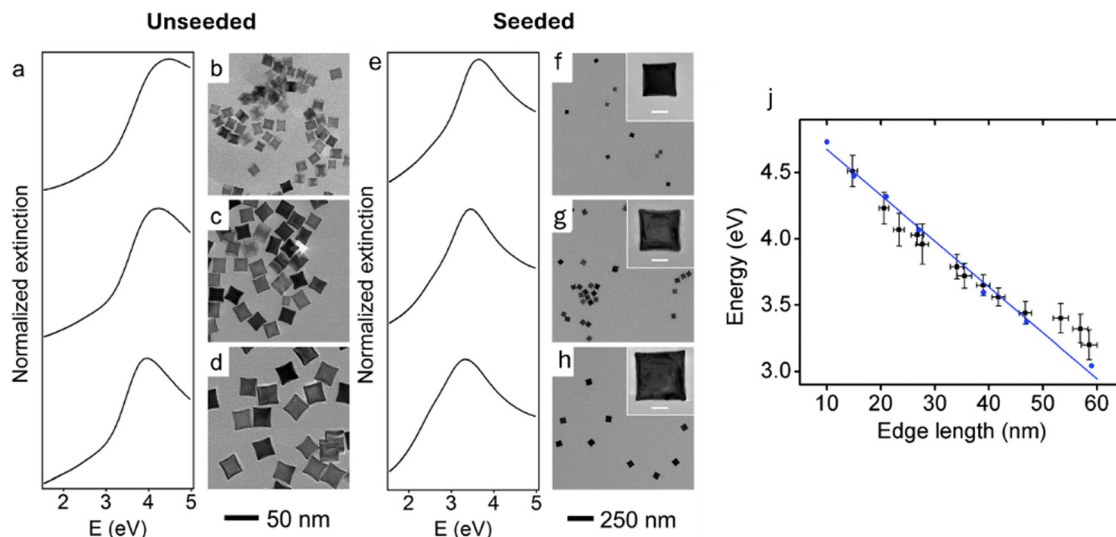
Fig. 1 (a) and (e) Experimental UV-vis extinction spectra of monodisperse Rh NCs in ethanol with corresponding TEM images from unseeded/seeded slow-injection methods of average edge lengths of (b) 15, (c) 21, (d) 27, (f) 39, (g) 47, and (h) 59 nm. The scale bars for the inset images in (f)–(h) are 20 nm. (j) The relationship of edge lengths and LSPR energies from experimental measurements (black squares) and numerical simulations (blue circles) of Rh NCs in ethanol. Reproduced and adapted from ref. 8 with permission from the Royal Society of Chemistry.
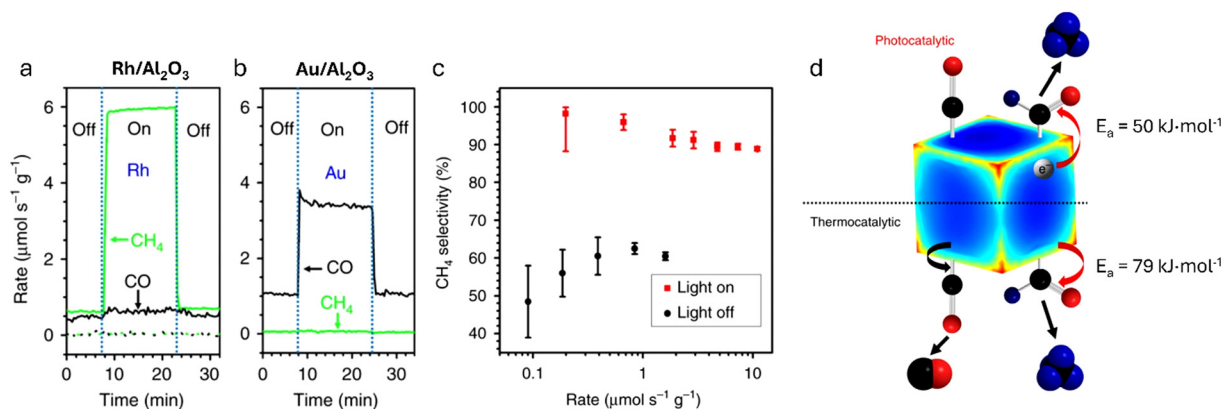

Fig. 2 Rates of CH_4 (green) and CO (black) production at 623 K on (a) Rh/Al_2O_3 (solid lines) and Al_2O_3 (dotted lines) under dark and ultraviolet illumination at 3 W cm^{-2}, and (b) Au/Al_2O_3 under dark and white light illumination at 3 W cm^{-2}. (c) Selectivity towards CH_4 as a function of overall reaction rates in dark (black circles) and under ultraviolet light at 3 W cm^{-2} (red squares). (d) The reaction mechanism for both plasmonic photocatalysis and thermocatalysis on the Rh NCs. The black, red, and blue spheres are carbon, oxygen, and hydrogen atoms. The red corners of the cube show the intense electric field from the excitation of LSPRs. Reproduced and adapted from ref. 9.

range showed the selectivity for CH_4 exceeding 95% under 3 W cm^{-2} UV illumination compared to darkness (Fig. 2c).

The detailed photocatalytic and thermocatalytic CO_2 reduction mechanisms illustrated the selective production of CH_4 over CO under light illumination (Fig. 2d). In thermocatalytic reactions, phonons activate both CHO and CO intermediates, producing CH_4 and CO with similar rates. In contrast, in photocatalytic reactions, the hot electrons generated from excited plasmonic Rh NCs selectively activate CHO intermediates

on the NC surface, accelerating CH_4 production with reduced activation energy. During the experiments, we observed an increased CH_4 production rate during photocatalytic reactions as the UV light intensity increased. However, we could not conclude whether the rate enhancement was due to hot carrier generation or photothermal heating, as we did not record the surface temperature in this early study in 2017. Therefore, to better understand the role of hot carriers in the system and isolate the effects of nonthermal and photothermal effects, our group,

along with numerous other scientists in the field, spent significant effort solving these mysteries.[10–13]

To obtain a complete thermal profile of the reaction environment, we improved the reactor setup and embedded two additional thermocouples, measuring the catalyst's top and bottom surface temperatures.[14] To accurately and quantitatively characterize the non-uniform thermal gradient in the catalyst bed, we proposed the calculation of "equivalent temperature", T_e, to simplify the entire thermal profile, which is

independent of E_a. Therefore, the production rate generated from thermal effects could be calculated as R_t, and the nonthermal production rate can be obtained by subtracting the total production rate from the thermal one ($R_{nt} = R_{tot} - R_t$). Applying our well-studied Rh NC on Al_2O_3 in the CO_2 reduction system, we quantitatively isolate the R_{nt} and R_t under different thermal conditions. Both the enhanced CH_4 production rate and high selectivity indicate the advantages of Rh nanosphere/TiO_2 as a superior plasmonic-enhanced photocatalyst compared to the Rh NC on Al_2O_3. The potential nonthermal contribution from the Rh–TiO_2 catalysts further complicated the catalytic process, motivating us to investigate this further.

We then focused on the separation between thermal and nonthermal contributions in plasmonic photocatalysis and developed two additional methods, namely the cover vs. uncover method[15] and the mass-dependent method.[16] For the cover vs. uncover method, a layer of inert, non-photocatalytic Ti_2O_3 was added on top of the active catalyst. This material acted as a photothermal material, absorbing light and converting light energy into heat without exciting the Rh NPs to generate hot electrons (Fig. 3a). Consequently, this configuration enabled the reactor system to exhibit only photothermal activity. By maintaining the same temperature profile, T_e, and comparing the reaction rates of the uncovered catalyst (exhibiting both thermal and nonthermal effects) and the Ti_2O_3-covered catalyst (showing only photothermal effects), the nonthermal contributions could be accurately extracted through subtraction (yellow shadowed area in Fig. 3b). On the other hand, the mass-dependent method aims to measure the nonthermal effect directly from the experiments by isolating the top illuminated surface layer of the catalyst (Fig. 3c).[16] In our experimental setup, only the surface layer of the catalyst within the light's penetration depth can experience both nonthermal and local photothermal effects. In contrast, the remaining catalyst inside the reactor contributes solely to the overall reaction through photothermal and external heating effects. We assumed that the photothermal effects would penetrate the catalyst bed systematically. As a result, there should be a consistent relationship between the thickness of the catalyst and the photothermal contributions (Fig. 3d). Based on this mass-dependent characteristic of thermal contributions, we proposed an innovative method to extract the nonthermal rate from the total rate enhanced by light using a curve fitting method to obtain the light contributions at zero thickness, which can be considered as the total nonthermal contribution. More importantly, the measurement of both thermal and nonthermal contributions in plasmonic catalysis as a function of temperature has made us realize that the earlier studies in this research field, which used quantum efficiency to characterize the activity of the catalyst, are misleading, as the total effects are a combination of thermal and nonthermal contributions. To more accurately measure the effect of light,
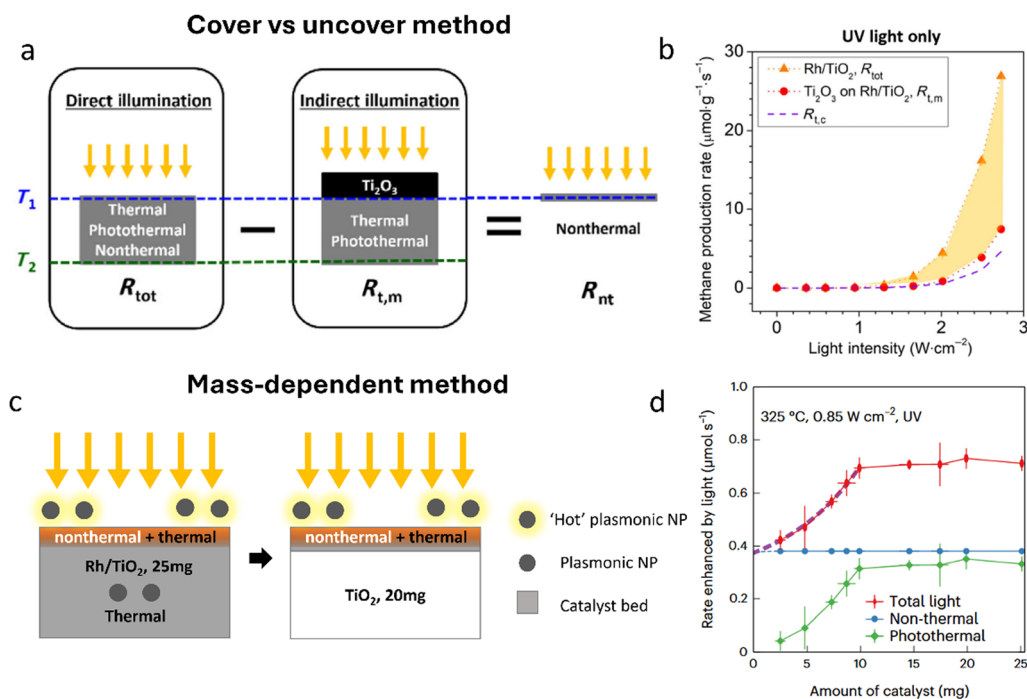

Fig. 3 (a) Schematic diagram of the cover and uncover method. (b) Measured total CH_4 production rate (R_{tot}) for unheated, UV light only is shown as a function of UV light intensity. Calculated ($R_{t,c}$) thermal CH_4 production rates are based on corresponding T_e. Measured ($R_{t,m}$) thermal CH_4 production rate from indirectly illuminated Rh/TiO_2 for identical T_1 and T_2 temperatures. The yellow shaded region represents the nonthermal contribution. Reproduced and adapted from ref. 15. (c) Schematic diagram of the catalyst bed and the mass-dependence test. (d) The calculated light-enhanced rate, the nonthermal rate, and photothermal rates under 325 °C, 0.85 W cm^{-2} UV light, with different amounts of catalysts in the reactor. Reproduced and adapted from ref. 16.

we proposed a new index, total light effectiveness, as a measure of the activity of catalysts under light illumination. This new index is a more accurate and useful indicator for researchers to discover more efficient plasmonic catalysts in their research.[16]

Since the novel Rh NC synthesis method was published in 2016, it has built the foundation for research in UV plasmonics. Wakita and Yao reported the magneto-optical properties of Rh NCs using magnetic circular dichroism (MCD) spectroscopy as a powerful tool to analyze the broad absorption peak in the UV region.[17] Their work provided more information for monitoring plasmonic responses and assigned transitions for excited Rh NCs, nanomultipods, and nanotetrahedra. These results indicate that size- and/or morphology-dependent interband transitions of rhodium contribute to their responses in the MCD spectra. Moreover, Xu and colleagues reported the enhanced light-emitting intensity of the polariton LED by depositing Rh NCs on ZnO microwire.[18] The device configuration was designed as n-RhNCs@ZnO MW/p-GaN, and the deposition of the synthesized Rh NCs on ZnO MW can lead to a significant increase in the light output of the as-fabricated LEDs due to the plasmonic-enhanced strong exciton–polariton coupling interaction.

A recent application demonstrated the nanoantenna's ability to enhance the UV autofluorescence of label-free streptavidin and hemoglobin proteins through Rh NC dimers, as reported by Roy and colleagues.[19] The designed Rh nanogap antennas showed a significant enhancement of autofluorescence brightness per protein by up to 120-fold, with detection volumes in the zeptoliter range and subnanosecond autofluorescence lifetime. After all, these works all applied Rh NCs made from our developed synthesis method and advanced our understanding in the field of UV plasmonics.

In summary, our interest in Rh and UV plasmonics began in 2015,[5] and the paper published in *Nanoscale Horizons* in 2016[8] paved the way for consistently synthesizing rhodium nanostructures in controllable sizes, shapes, and extinction spectra. The synthesized Rh NCs enabled selective CO_2 reduction to CH_4, achieving over 95% selectivity, attributed to strong UV plasmonic enhancement.[9] To improve performance, we optimized the catalyst architecture from Rh NCs/Al_2O_3 to Rh NSs/TiO_2, leading to higher production rates and improved apparent quantum efficiency.[14] To further understand the light–matter interaction, we developed the cover/uncover method in 2020[15] and the mass-dependence method in 2023[16] to differentiate hot carrier contributions from photothermal effects. These advanced methods provide more effective ways to investigate the contributions from both light effects under various reaction conditions. Probably most importantly, the new parameter we proposed, overall light effectiveness, can be viewed as a comprehensive metric for evaluating light effectiveness in plasmonic-involved systems. This publication in *Nature Catalysis*[16] has been cited many times by researchers in the field since it was published at the end of 2023.

Looking back on the journey, it can be said that the paper published in *Nanoscale Horizons* sets the stage and guides our path in the field of plasmonic photocatalysis. Over the past decade, *Nanoscale Horizons* has established a reputation as one of the leading journals in nanoscience and nanotechnology, publishing high-quality, cutting-edge papers. On this special 10th anniversary, we celebrate its remarkable achievements and look forward to another decade of groundbreaking science in *Nanoscale Horizons*. We extend our warmest congratulations to the Editorial Board and wish them continued success in leading the journal to greater heights.

Conflicts of interest

There are no conflicts to declare.

Acknowledgements

References

1 K.-S. Lee and M. A. El-Sayed, *J. Phys. Chem. B*, 2006, **110**, 19220–19225.

2 J. M. Sanz, D. Ortiz, R. Alcaraz de la Osa, J. M. Saiz, F. González, A. S. Brown, M. Losurdo, H. O. Everitt and F. Moreno, *J. Phys. Chem. C*, 2013, **117**, 19606–19615.

3 D. M. Arboleda, V. Coviello, A. Palumbo, R. Pilot and V. Amendola, *Nanoscale Horiz.*, 2025, **10**, 336–348.

4 V. Jain, R. K. Kashyap and P. P. Pillai, *Adv. Opt. Mater.*, 2022, **10**, 2200463.

5 A. M. Watson, X. Zhang, R. Alcaraz de la Osa, J. M. Sanz, F. González, F. Moreno, G. Finkelstein, J. Liu and H. O. Everitt, *Nano Lett.*, 2015, **15**, 1095–1100.

6 S. Xie, X. Y. Liu and Y. Xia, *Nano Res.*, 2015, **8**, 82–96.

7 A. J. Biacchi and R. E. Schaak, *ACS Nano*, 2015, **9**, 1707–1720.

8 X. Zhang, P. Li, Á. Barreda, Y. Gutiérrez, F. González, F. Moreno, H. O. Everitt and J. Liu, *Nanoscale Horiz.*, 2016, **1**, 75–80.

9 X. Zhang, X. Li, D. Zhang, N. Q. Su, W. Yang, H. O. Everitt and J. Liu, *Nat. Commun.*, 2017, **8**, 14542.

10 R. Verma, G. Sharma and V. Polshettiwar, *Nat. Commun.*, 2024, **15**, 7974.

11 E. Cortes, L. V. Besteiro, A. Alabastri, A. Baldi, G. Tagliabue, A. Demetriadou and P. Narang, *ACS Nano*, 2020, **14**, 16202–16219.

12 G. Baffou, I. Bordacchini, A. Baldi and R. Quidant, *Light: Sci. Appl.*, 2020, **9**, 108.

13 A. J. Offen, Z. Geng, Y. Yu and J. Liu, *ACS Appl. Energy Mater.*, 2023, **6**, 11762–11772.

14 X. Zhang, X. Li, M. E. Reish, D. Zhang, N. Q. Su, Y. Gutiérrez, F. Moreno, W. Yang, H. O. Everitt and J. Liu, *Nano Lett.*, 2018, **18**, 1714–1723.

15 X. Q. Li, H. O. Everitt and J. Liu, *Nano Res.*, 2020, **13**, 1268–1280.

16 Z. Geng, Y. Yu, A. J. Offen and J. Liu, *Nat. Catal.*, 2023, **6**, 1241–1247.

17 T. Wakita and H. Yao, *Chem. Phys. Lett.*, 2021, **779**, 138866.

18 H. Xu, C. Miao, M. Jiang, Y. Liu, C. Kan and D. Shi, *J. Lumin.*, 2021, **235**, 118016.

19 P. Roy, S. Zhu, J.-B. Claude, J. Liu and J. Wenger, *ACS Nano*, 2023, **17**, 22418–22429.